PASSIVE TORQUE SIMULATION OF SMALL ANGULAR CONTACT BEARING AT HIGH SPEED

JOSEF KEKULA, JAN SMOLIK, MATEJ SULITKA
Czech Technical University in Prague
Faculty of Mechanical Engineering
Department of Production Machines and Equipment
Prague, Czech Republic

e-mail: j.kekula@rcmt.cvut.cz

In order to predict heat generation in super precision ball bearings at high speeds the Harris and Houpert frictional models were applied to a high speed range with maximum speed of 150 000 RPM. The measurement of thermal behaviour in super precision ball bearings was observed on a high speed spindle for micromilling. Outer ring bearing temperature and torque was measured simultaneously under stable lubrication conditions set by the oil-air lubrication unit. Measurement was performed via our custom built non-driven spindle on a special test rig. The complex thermo-mechanical model of the spindle unit was used to determine high speed spindle behaviour on super precision high speed ball bearings. Torque models were compared with experimental data and its deviation from real torque was observed. Following our testing this proposal to modify the Houpert torque model was designed.

KEYWORDS

NOMENCLATURE

a	major semi-axe of the contact ellipse
b	minor semi-axe of the contact ellipse
D	diameter
E_A, E_B	Young´s modulus of contact materials
f_o	factor dependent on the bearing lubrication type (considered as 0.001 for oil-mist)
d_m	pitch diameter of the bearing
T_B	temperature of the rolling elements
f_i	this factor depends on type of bearing design and its relative loading
F_β	involves the magnitude and direction of the applied load
d_m	pitch diameter of the bearing
z, y	is dependent on the bearing design
v	average velocity between contact surfaces
F_S	the static equivalent load
Q	normal contact force of the relevant contact
C_S	static loading capacity
F_C	Centrifugal force
B	width of the bearing
M	torque
Z	number of rolling elements
α	current contact angle
μ	frictional coefficient
ω	rotational velocity
η	dynamic viscosity
ν	lubricant kinematic viscosity

INDEX

i, o	inner, outer
l	rolling
m	index of cage velocity
pc	point contact
T	total torque
v	viscous
s	spin
x	perpendicular direction to the bearing rotational axis
HSSB	high speed small bearing

1. INTRODUCTION

Heat generation of high-speed super precision ball bearings in machine tool spindles can cause undesirable changes of spindle dimensions. This effect can produce workpiece dimensional errors, especially in micromilling operations. In micromilling the highest speed levels of tools are achieved, therefore prediction of heat generation is particularly important. Overheating the bearing and its surrounding structure can lead to shortening of bearing life or, in fatal cases, bearing seizure. In order to predict the thermal behaviour of the spindle structure is important to know the bearing thermal properties at operational speed.

2. BEARING MODEL

This model of the angular contact bearing is based on the Harris theory [HARRIS, 1966]. This model provides a fundamental description of changes in internal geometry when the bearing is brought to speed.
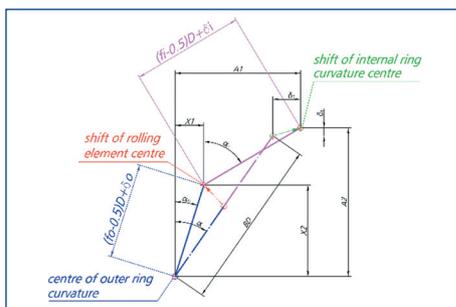

Figure 1. Change in internal geometry of the angular contact bearing after centrifugal effects are applied (the centre of outer race curvature is considered as static)

The Harris model assumes axisymmetric loading and behaviour of the bearing. Angular contact rolling bearing represent a complex system which changes its properties depending on the current speed and external loading.

Fig. 1. compares the initial state of internal bearing geometry with the final state when speed is applied. Thanks to this description it is possible to observe the internal bearing geometry change. As presented in Fig. 1, the Harris model is derived from geometrical relationships and Hertz contact theory. The next important element is detailed knowledge of the internal kinematics of the bearing.

Application of the axisymmetric model of the bearing the description of its properties is possible. This description is made for arbitrarily chosen inputs parameters (independent variables). Unknown parameters are:

internal contact angles, contact forces, axial shift of bearing rings (in case of constant preload task), overall internal kinematics of the bearings, axial and radial stiffness and contact ellipses dimensions. As input parameters serves speed, preloading force and material parameters of bearing rings and rolling elements. This system of equations is solved thanks to the Newton iteration method as presented in [HOLKUP, 2007].

3. TORQUE MODELS

The outputs of the bearing model are used in torque models. This approach allows simulations of torque with internal force current values, geometrical and contact parameters. The most widely known torque model of rolling bearing is the model presented by Harris [HARRIS, 1966]. This model is built on the Snare [SNARE, 1968] and Palmgren [PALMGREN, 1959] investigations. Houpert provides further detailing of the torque model [HOUPERT, 1999].

3.1 HARRIS MODEL

The Harris torque model considers three main components of final torque. The first is torque due to applied load, the second is viscous friction torque, and finally the third is torque due to spinning of rolling elements. In general form this model considers the type of bearing (contact angle), type of lubricant (grease or oil) and manner of lubrication (oil mist or oil bath). Types of the bearing and type of the lubrication are introduced by empirically coefficients.

3.1.1. Rolling resistance

This torque component is used for rolling resistance, with the following relationship (inner and outer contact) as per this model:

$$M_{l_{i,o}} = \frac{1}{2} \cdot 0,001 \cdot \left(\frac{0,46 \cdot Q_{i,o} \cdot \sin \alpha_{i,o}}{C_S}\right)^{\frac{1}{3}} \cdot 3 \cdot Q_{i,o} \cdot \sin \alpha_{i,o} \cdot d_m \qquad (1)$$

It is necessary to properly distribute the component for each contact. This distribution is performed according to Jorgensen (JORGENSEN, 1997). The rolling resistance torque component is divided into halves for each contact (i-inner/o-outer).

3.1.2 Viscous friction torque

This torque component is the most important; especially for small high-speed bearings. For the viscous component the following can be written in accordance with Jorgensen:

$$M_{vi} = M_{vo} = \frac{M_v}{2} = 0,225 \cdot 1.10^{-3} \cdot (\nu(T_B) \cdot \omega)^{\frac{2}{3}} \cdot d_m^3 \qquad (2)$$

It is important to realize that lubricant viscosity is strongly dependent on temperature. In this view it is necessary to consider current viscosity. Viscosity value can be actualised according to the current bearing temperature. If a false temperature is considered significant errors can be returned.

3.1.3 Spin of rolling elements:

$$M_{S\,i} = \frac{3 \cdot \mu \cdot Q_i \cdot a_i \cdot \varepsilon}{8} \qquad (3)$$

In this model the spinning component is considered only at inner contact because the outer contact is assumed as leading contact.

Final torque acting to the shaft (to inner ring) is considered as the sum of individual components:

$$M_T = M_{l\,i,o} + M_{v\,i,o} + M_{S\,i} \cdot \sin \alpha_i \qquad (4)$$

3.2 HOUPERT MODEL

The Houpert model provides a more analytical approach. This model describes forces and moments which act upon the rolling elements (balls). Detailed calculations are based on contact analysis of the balls and rolling race. At the contact zone the slip velocities distribution are considered. A knowledge of detailed contact geometry is necessary. The dimensions of the current contact ellipses and detailed dimensions of the rolling races are required to execute this calculation. Nevertheless there is used several empirical coefficients as in the Harris model.

In general the final torque is divided to similar components as per the Harris model. There is hydrodynamical resistance, rolling resistance, curvature shape and resistance caused by pivoting effects.

3.2.1 Rolling resistance

Knowledge of Snare is required to execute this calculation (SNARE, 1968). In [HOUPERT 2002]. Houpert adjusts Snare's relationship by considering the variation of the maximum value of the frictional coefficient in the contact zone. Introduction of an equivalent frictional coefficient to Snares relationship (HOUPERT, 2002) gives this component for both contacts as:

$$MER_{i,o} = 42.10^{-5} \cdot Q_{i,o} \cdot R_{x\,i,o} \cdot \frac{\mu_e}{0.11} \qquad (5)$$

3.2.2 Hydrodynamic resistance:

Hydrodynamic resistance torque component describes the internal viscous force acting upon the rolling element. It is possible to express viscous force by considering different lubrication regimes in the contact. In general it is possible to account for a variety of lubrication regimes between the rolling element and rolling race.

PVE (piezo-viscous-elastic). This regime is known as elasto-hydro-dynamic lubrication (EHL). In an EHL regime the elastic deformation of rolling elements and races influences the thickness of lubricant film. The pressure in the contact influences viscosity of the lubricant. A number of relationships for calculating the viscous force acting to the ball are possible. Several formulas are presented in the following section.

Hamrock's: formula presented in [HOUPERT, 1985]:

$$FR_{pc\,i,o} = 2,86 \cdot E^* \cdot R_{x\,i,o}^2 \cdot k_{i,o}^{0,348} \cdot G_{i,o}^{0,022} \cdot U_{i,o}^{0,66} \cdot W_{pc\,i,o}^{0,47} \qquad (6)$$

Houpert's formula (BALAN et. al., 2013):

$$FR_{EHL\_H} = 2,765 \cdot E^* \cdot R_{x\,i,o}^2 \cdot k_{i,o}^{0,35} \cdot U_{i,o}^{0,656} W_{i,o}^{0,466} \cdot G_{i,o}^{0,022} \cdot \qquad (7)$$

Biboulet's formula (BALAN et. al., 2013):

$$FR_{EHL\_B} = 7,5826 \cdot E^* \cdot R_{x\,i,o}^2 \cdot k_{i,o}^{0,405} \cdot U_{i,o}^{3/4} W_{i,o}^{1/3} \qquad (8)$$

Where:
Equivalent Young's modulus:

$$E^* = 2 \cdot \left(\frac{1 - \mu_A^2}{E_A} + \frac{1 - \mu_B^2}{E_B}\right)^{-1} \qquad (9)$$

Hertzian radius of the curvature of the elastic contact:

$$R_{x\,i} = \frac{D_b}{2} \cdot \left(1 - \frac{D_b \cdot \cos \alpha_i}{d_m}\right) \qquad (10)$$

$$R_{x\,o} = \frac{D_b}{2} \cdot \left(1 + \frac{D_b \cdot \cos \alpha_o}{d_m}\right) \qquad (11)$$

Reduced radius ratio for inner contact:

$$\overline{k_i} = \frac{1 + \overline{K_i}}{\overline{K_i}} \cdot \frac{1}{1 - \frac{D_b \cdot \cos \alpha_i}{d_m}} \qquad (12)$$

Reduced radius ratio for outer contact:

$$\overline{k_o} = \frac{1 + \overline{K_o}}{\overline{K_o}} \cdot \frac{1}{1 + \frac{D_b \cdot \cos \alpha_o}{d_m}} \qquad (13)$$

K parameter defining race curvature radius – the race curvature radius r is function of this parameter as follows:

$$r_{i,o} = \left(1 + \overline{K_{i,o}}\right) . \frac{D_b}{2} \tag{14}$$

Dimensionless speed parameters are defined as:

$$U_{i,o} = \frac{\eta_0 . v_{m\,i,o}}{E^* . R_{x\,i,o}} \tag{15}$$

Dimensionless load parameter:

$$W_{i,o} = \frac{Q_{i,o}}{E^* . R_{x\,i,o}^2} \tag{16}$$

Dimensionless material parameter:

$$G_{i,o} = \alpha_p . E^* \tag{17}$$

The pressure-viscosity coefficient is dependent on the type of lubricant. In the torque model the following relationship was used. The temperature dependence in this relationship is maintained due to kinematic viscosity.

$$\alpha_p = s . v^t . 10^{-9} \tag{18}$$

Where s and t are lubricant coefficients. The hydrodynamic rolling resistance component is computed for each contact (inner/outer) according to the current operational conditions. As a relevant model the EHL regime was chosen because viscosity of the lubricant influences the lubrication regime. If a lubricant with a dynamic viscosity about 0,350 Pa.s is used the IVR (isoviscous rigid) regime is dominant in the contact. For lubricants with viscosities in a range between 0,02 and 0,08 Pa.s the EHL regime is dominant in the contact. All models of viscous forces are derived for full film lubrication.

3.2.3 Curvature shape and pivoting resistance
Houpert consider curvature of the contact area in spaces where additional braking moment is generated. Curvature of this effect approximates as parabola. If there are conditions for two rolling lines in the contact [HOUPERT, 2002] it can be written:

$$MC_{i,o} = 0{,}0806 . \mu . Q_{i,o} . \frac{a_{i,o}^2}{R_{a\,i,o}} . f_{c\,i,o} \tag{19}$$

$$MP_{i,o} = \frac{3}{8} . \mu . Q_{i,o} . a_{i,o} . f_{p\,i,o} \tag{20}$$

Where f_c a f_p are curvature and spin coefficients. These coefficients are dependent on the single parameter E as described Houpert in [HOUPERT, 1999]. R_a is Hertzian radius of curvature.

3.2.4 Final torque
The contribution of one rolling element on the inner ring it is possible to calculate according to Houpert as:

$$dM_T = 2 . (FR_i + FR_o) . \frac{r_o . r_i}{d_m} + \frac{MC_i . r_o + MC_o . r_i}{D_b} + \frac{MER_i . r_o + MER_o . r_i}{D_b} + \frac{MP_i . \left(1 + \frac{D_b . \cos\alpha_i}{d_m}\right)}{2} . \sin\alpha_i \tag{21}$$
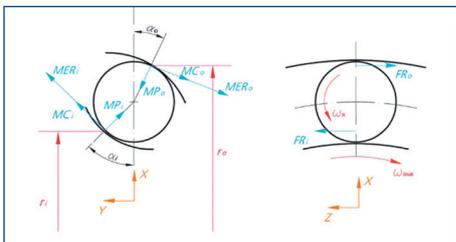
Figure 2. Moments and forces acting to the rolling element

Final torque acting to the inner ring of the bearing (shaft) is given as sum of all rolling elements:

$$M_T = Z . dM_T \tag{22}$$

4. SIMULATION MODEL
Torque models were programmed in Matlab software. The bearing model described was extended by torque outputs. Final torque is calculated for current contact angles and contact forces for given initial conditions.

The simulation accounting for defined initial parameters – bearing geometry (external dimensions and curvature of rolling races), material properties (Young modulus, density), range of preloading forces, speed range, radial deformation value, temperature of bearing and lubricant viscosity model.
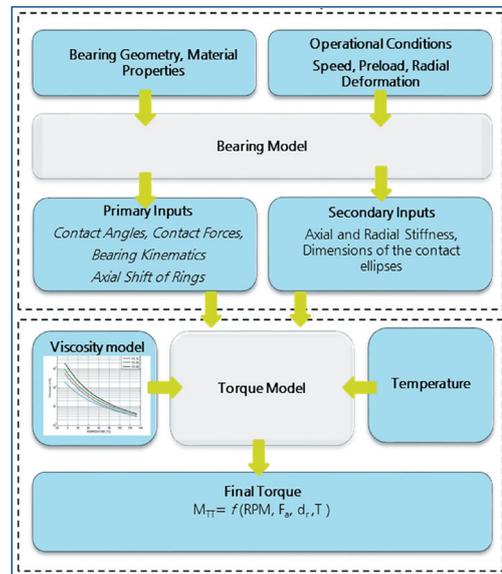
Figure 3. Bearing torque simulation model

If the complete task is defined the final torque is computed according to the torque models mentioned above. Final torque is always composed from individual contributions arising from the contact area on the inner or outer ring. The torque model scheme can be seen from Figure 3. As the temperature input serves temperature of outer ring. The whole model is ready for its use in transient complex simulation. A complex simulation provides the proper heat source of the bearing. In a complex simulation the time dependency of the thermal field is considered by considering the current surrounding structure deformations.
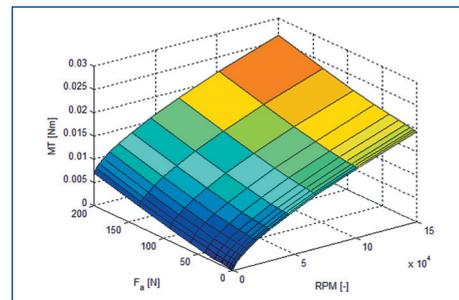
Figure 4. Final torque –Harris model, oil VG68, constant temperature 40 °C, axial preload 50 N, without radial deflection 0 mm

Character of final torque according to the individual torque model is in Fig. 4 and Fig. 5.
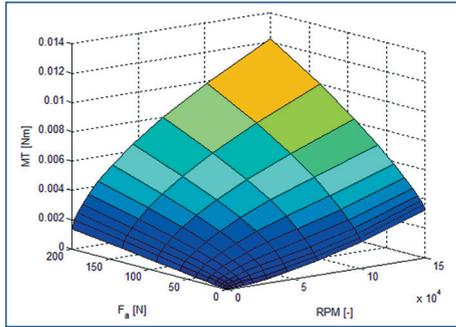
Figure 5. Final torque – Houpert model, EHL lubrication model, oil VG68, axial preload 50 N, constant temperature 40 °C, without radial deflection 0 mm

Presented results are performed for SKF 71900 CE/HCP4A bearing, with 50 N axial preload without radial deflection. VG 68 oil and a constant temperature of 40 °C are considered. From this comparison it can be seen that characters of this models are different. The Houpert model brings more sensitive behaviour to the axial loading of the bearing. Differences in absolute values of the final torque are also apparent. Experimental verification at high speed areas are needed. This measurement will be performed for an examined bearing. The torque and temperature will be captured in order to compare these models and experimental results.

5. EXPERIMENTAL SETUP

Experimental setup was performed on a couple of high speed additional spindles. The spindles were designed by the author as prototypes for micro milling. Maximum speed achieved is 150 000 RPM with a compressed air driven turbine. One of the spindles is powered and the second is driven. On the driven spindle torque is measured as a reaction torque of the bearings. The experimental setup is shown in Fig. 6. The two high speed spindles are placed vertically against each other. Spindles are placed in a special test rig which holds them precisely in position. In the lower position the powered spindle (12) is fixed to the base of test rig (6). The compressed air supply is delivered to the turbine via a feeding hose (11). The upper spindle is fixed through the torque sensor to the test rig cantilever (1). Both spindles are centred precisely. The join of both spindles is performed by flexible damped
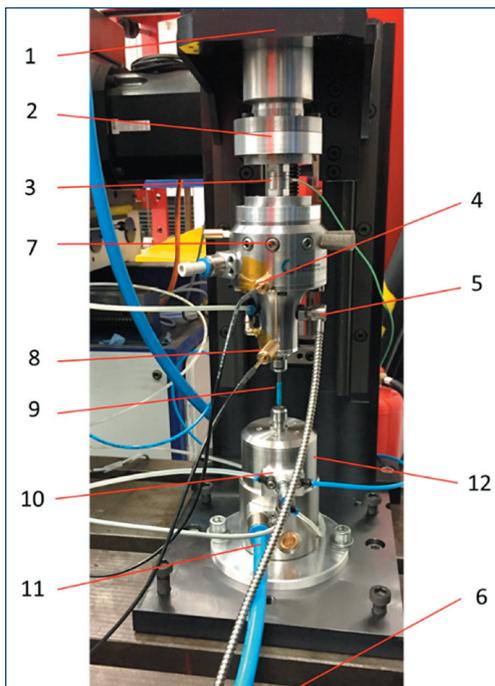

Figure 6. Experimental setup

clutch (9). The speed is controlled via a speed probe (10) and speed feedback control. Outer ring thermometers (4 and 8) are placed on the spindle to be measured. Rotor vibrations are checked by an installed accelerometer (5).

The spindles have identical angular contact hybrid bearings. The front bearing of the spindle shaft is SKF 71900 CE/HCP4A with middle diameter 16 mm and SKF 707 CE/HCP4A with middle diameter 13 mm. Speed range is chosen from 10 to 150 thousands RPM.

The preloading force is changed with pressure variation in the special preload mechanism inside the spindle. Three levels of force was applied – 12; 26 and 50 N. Pressure applied was 1.5; 3 and 5 bar.

The bearings are lubricated by an oil-air system. The VG68 viscosity oil Shell Omala was used. Lubrication amount was 5.10^{-3} g/hour for each bearing per manufacturer recommendation.

6. TEST PROCEDURE

Each measurement starts from a cooled down state – every part of the spindle has the same temperature as the surrounding air. Temperature recording is continuous at 1 Hz period. After acceleration to the specified level of speed and thermal stabilization of structure the torque measurement is performed. During torque measurement the shaft is decelerated to an idle state. The resulting torque is evaluated as the difference between idle state and state at certain speed. Thus the measured torque is captured at real conditions in spindle structure. Each speed and force level was three times repeated. The final uncertainty was determined from number of measurement and from precision of used gauges. The uncertainty is projected to the final result (see Fig. 10).

7. RESULTS

The bearing model and torque models were programmed in the Matlab environment. Torque can be observed for different operational states. Each torque model was compared (see Fig. 7). In Fig. 7. the experimental data was presented (black line). The closest is the Houpert model with its own description of viscous force (see equation (6)) and the same model with Hamrock's viscous force formula (see equation (5)). Presented (Fig. 7)
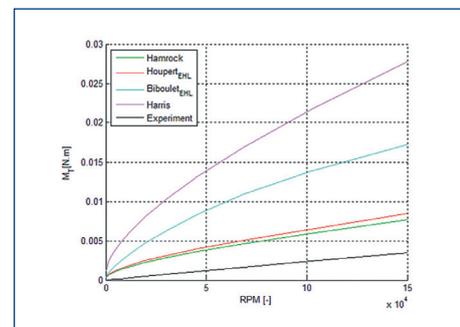

Figure 7. Torque model comparison; SKF 71900 CE/HCP4A, oil VG68, constant temperature 32 °C, axial preload 50 N, bearing radial deformation 0 mm
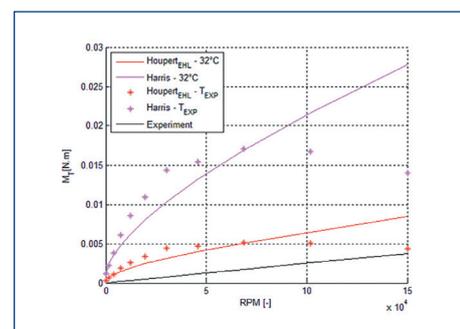

Figure 8. Torque models comparison, SKF 71900 CE/HCP4A, oil VG68, variable temperature according measurement conditions, axial preload 50 N, bearing radial deformation 0 mm

torque model comparison with experimental data was not performed correctly because experimental values were captured under different temperature conditions. Thus this comparison is only for illustrative purposes. Still, it can be seen that the Harris model greatly exceeds the experimental data. The Houpert's model with Biboulet's EHL model of viscous force is not proper too.

For a relevant comparison of the models the temperature must be considered according to the experimental data. Temperature influences the lubricant viscosity and thus the resulting torque. If a similar comparison is performed with full consideration of the temperature effect the following data are observed (see Fig. 8).

From this comparison it is obvious that the compared torque models are inappropriate at extreme speed applications in small bearings. Comparison of both models (Harris and Houpert) for examined bearing at 50 N axial preload is presented in Fig. 8.

This comparison is correct in view of proper temperatures. Experimental data was compared with Houpert's model. Comparison was performed by the ratio between experimental and theoretical values. This ratio is a speed dependent value, presented as a reduction factor for Houpert's model (see Fig. 9).

Ratios for different preloading forces have similar characters as shown in Fig. 10. If we take into account the uncertainties of experimental values the final reduction ratio lies in the certain area. From this area the final reduction factor was derived. This area is possible to see in Fig. 10.
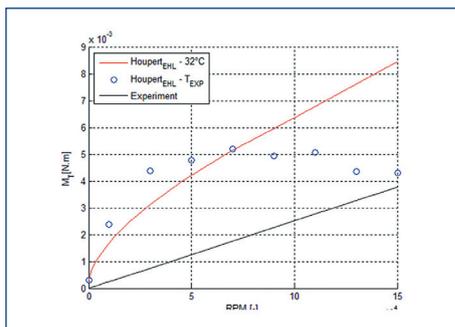

Figure 9. Experimental data and Houpert model data comparison. Preloading force 50N, bearing radial deformation 0 mm
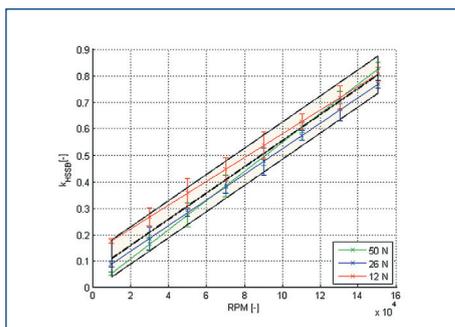

Figure 10. Experimental data and Houpert model data ratios of different preloading forces

From the area of differential preloading force ratios it is possible to see that uncertainties of performed measurements (error bars) are included.

The final reduction factor formula with uncertainty is suggested as:

$$k_{HSSB} = 4,95.10^{-6}.RPM + (0,06 \pm 0,07) \qquad (23)$$

The final torque calculation for small bearings and extreme speed operations M_{HSSB} is then possible to obtain as a product of Houpert model value and suggested reduction factor k_{HSSB}.

$$k_{HSSB} = 4,95.10^{-6}.RPM + (0,06 \pm 0,07) \qquad (23)$$

Validity of proposed reduction is for speed range $1.10^3 - 15.10^4$ RPM. Preloading force range is between $12 - 50$ N.
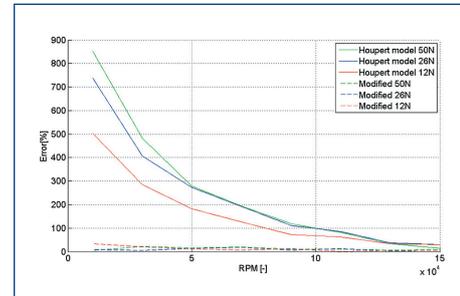

Figure 11. Houpert model and modified model errors

Errors of Houpert's model can reach an order of magnitude. For this reason it is recommended that Houpert's model be considered inappropriate for modelling extreme speed, small bearings rotor systems. This new proposal provides dependable results with satisfactory deviations for spindle design.

8. AN EXAMPLE OF A COMPLEX SIMULATION

Thanks to the complex thermal – mechanical simulation it is possible to describe all processes which act upon the bearing, especially temperature and surrounding structure deformation effects. The surrounding structure is modelled by the FE method. Using the bearing model calculating bearing behaviour at all operational states becomes possible. Outputs of the bearing model for certain input parameter ranges are stored as a database of bearing properties. As a property of the bearing the set of dependent variables on the independent input variables are considered.
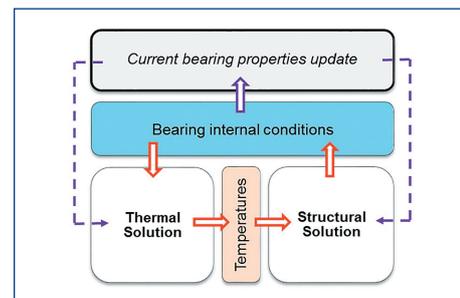

Figure 12. Complex thermal-mechanical simulation scheme

During the transient complex simulation current values of dependent parameters are interpolated from the database of the bearing. In a complex simulation the value of hydro-dynamical force is computed according to the current temperature, then the final value of torque is determined for the current step. Heat power is computed based on the knowledge of current speed and current torque in thermal task. One half of the heat power (Q/2 – see Fig. 13) is applied to the rolling element and the second half is applied to the bearing rings equally to the relevant nodes in the FE model.

Complex thermo-mechanical simulation of the spindle behaviour with angular contact hybrid bearings was performed. The Houpert torque model and its modification was applied. Boundary conditions are tuned according to the experimental setup for a certain speed level. From the measured torque the heat power was determined and applied to the FE model. The boundary conditions were tuned, especially natural and forced convections on the external and internal surfaces.
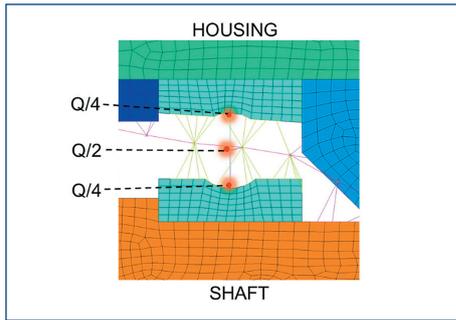
Figure 13. FE model of the bearing and its surroundings; Heat s application

The outer ring temperature was observed. The final match of measured and simulated temperatures can be seen in Fig. 14.
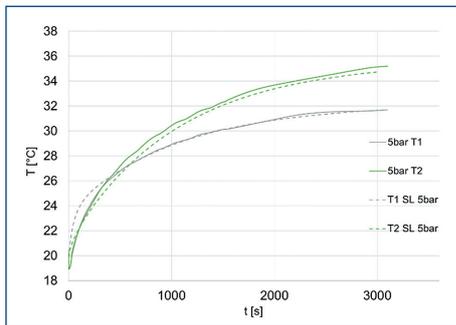

Figure 14. Tuning of boundary condition with experimental heat source data; match between experimental and simulated data -dotted line; front and rear bearing; 70 000 RPM; 50 N axial preload (preloading pressure 5 bar)

The whole model is built as 2D axisymmetric utilising the Ansys software in APDL (Ansys Parameter Design Language). The simulations at 70 000 RPM and 50 N of preloading force are presented. The results are shown in Fig. 13 and Fig. 14. Comparison of Houpert model and its modification with experimental data is shown in Tab. 1, 2, 3 and 4.
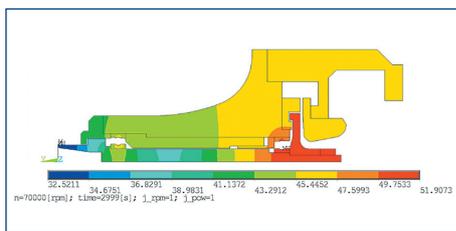

Figure 15. Thermal field after 3 000 s – Houpert model; 70 000 RPM; 50 N axial preload

M_T [N.mm]	Bearing 1	Bearing 2
Experimental	1.6	1.1
Model Houpert	3.1	1.9
Error [%]	88.4	72.1

Table 1. Torque results from performed simulation; 70 000 RPM; 50 N axial preload

T_{OR} [°C]	Bearing 1	Bearing 2
Experimental	31.7	35.1
Simulation	44.6	48.9
Error [%]	40.7	39.3

Table 2. Resulting temperatures of bearings from performed simulation, Houpert model, 70 000 RPM; 50 N axial preload
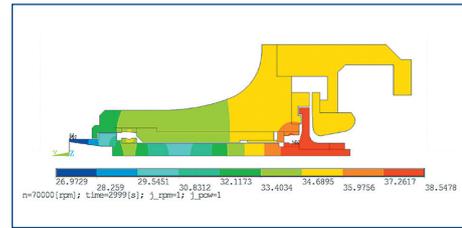

Figure 16. Thermal field after 3 000 s – Modified Houpert torque model; 70 000 RPM; 50 N axial preload

M_T [N.mm]	Bearing 1	Bearing 2
Experiment	1.6	1.1
Houpert modiff.	1.8	1.1
Error [%]	9.1	1.0

Table 3. Torque results from performed simulation – Houpert modification; 70 000 RPM; 50 N axial preload

T_{OR} [°C]	Bearing 1	Bearing 2
Experimental	31.7	35.1
Simulation	34.1	36.7
Error [%]	7.5	4.5

Table 4. Resulting temperatures of bearings from performed simulation – Houpert modification; 70 000 RPM; 50 N axial preload

From the presented results it is possible to see that the modified Houpert model is a satisfactory approach to the real state. Maximal error of the simulated torque is 9,1 % with 7,5 % thermal error. These errors are considered as satisfactory in transient complex tasks.

9. CONCLUSION

A comparison of bearing torque experimental data and simulated models was performed. Simulations and experiments were performed under extreme speed conditions for small angular contact bearings. The differences between modelled and experimental results were observed. A modification of the Houpert torque model for extreme speed levels and small bearings is suggested. Houpert's torque model and its modification was built into the complex simulation, thus temperature and surrounding structure effect was considered. The Houpert torque model modification is valid for a speed range of $1.10^3 - 15.10^4$ RPM and preloading force span between 12 – 50 N. The modification is valid for VG68 oil-air lubrication method with dosage at 5.10^{-3} g/hour. Force influence was not possible to observe from the experiments performed due to small force variation.

REFERENCE
[BALAN 2013] BALAN, M. R. et al., 2013. The influence of the lubricant viscosity on the rolling friction torque. Tribology international 72.
[BOSSMANNS 1999] BOSSMANNS, B.. T. J. F. Thermal model for high speed motorized spindles. International Journal of Machine Tools and Manufacture. 1999, vol. 39, pg. 1345-1366.
[HAMROCK 1994] HAMROCK, B. J., 1994. Fundalmentals of Fluid Film Lubrication. New York: Mc Graw-Hill, Inc.
[HARRIS 1966] HARRIS, T. A., 1966. Rolling bearing analysis. New York: John Wiley & Sons, Inc. 3rd edition.
[HOLKUP 2007] HOLKUP, T., 2007. Complex thermo-mechanical model of high speed bearings. Praha: ČVUT.
[HOUPERT 1985] HOUPERT, L. L. P., 1985. A Theoretical and experimental Investigation Into Rolling Bearing Friction. Lyon: Sborník Eurotrib Conference.

[HOUPERT 1999] HOUPERT, L., 1999. Numerical and analytical calculations in ball bearings. Toulouse: 8th Europen space mechanism and tribology symposium. Proceeding of the conference.

[HOUPERT 2002] HOUPERT, L., 2002. Ball Bearing And Tapered Roller Bearing Torque: Analytical, Numerical And Experimental Results. Houston: STLE Annual Meeting.

[HOUPERT 2002] HOUPERT, L., 2002. Ball Bearing And Tapered Roller Bearing Torque: Analytical, Numerical and Experimental Results. Houston: 57th STLE Annual Meeting.

[JORGENSEN 1997] JORGENSEN, B. R.. S. Y. C., 1997. Dynamics of machine Tool spindle/bearing systems under thermal growth. Journal of Tribology, Transactions of the ASME. vol. 119, pg. 875-882, School of Mechanical Engineering, Purde Iniversity.

[PALMGREN 1959] PALMGREN, A., 1959. Ball and roller engineering. 3rd edition, Philadelphia: Burbank.

[SNARE 1968] SNARE, B., 1968. Rolling Resistance in Loaded Ball Bearing. Ball Bearing Journal, s. 158.

CONTACTS

Ing. Josef Kekula
Ing. Jan Smolik, Ph.D.
Ing. Matej Sulitka, Ph.D.
Czech Technical University in Prague, Faculty of Mechanical Engineering
Department of Production Machines and Equipment
Horska 3, 128 00 Prague, Czech Republic
e-mail: j.kekula@rcmt.cvut.cz, www.rcmt.cvut.cz